Lasing properties from dye-doped holographic polymer dispersed liquid crystal confined in two-dimensional cylindrical geometry

Jie Zhang,[1] Haitao Dai,[1,*] Chao Yan,[2,3] Degang Xu,[2,3] Yanjun Liu,[4] Dan Luo,[5] and Xiaowei Sun[5]

[1]*Tianjin Key Laboratory of Low Dimensional Materials Physics and Preparing Technology, School of Science, Tianjin University, Tianjin 300072, China*

[2]*Institute of Laser and Optoelectronics, College of Precision Instrument and Optoelectronic Engineering, Tianjin University, Tianjin 300072, China*

[3]*Key Laboratory of Optoelectronic Information Science and Technology (Ministry of Education), Tianjin University, Tianjin 300072, China*

[4]*Institute of Materials Research and Engineering, Agency for Science, Technology and Research (A*STAR), 2 Fusionopolis Way, Innovis, #08-03, Singapore 138634, Singapore*

[5]*Department of Electrical & Electronic Engineering, South University of Science and Technology of China, Shenzhen 518055, China*

htdai@tju.edu.cn

Abstract: In this paper, we investigate the lasing behavior of holographic polymer dispersed liquid crystals (H-PDLCs) filled in capillary tubes (CTs). The emission properties from CTs with various core diameters are explored experimentally. The experimental results show that the smallest threshold is 19.4 μJ/pulse in CTs III (300 μm) corresponding to the largest FWHM 0.42 nm. The minimum FWHM is 0.29 nm in CTs I (75 μm) corresponding to largest threshold 31.5 μJ/pulse. According to experimental results and theoretical analysis, the different lasing behaviors from various core diameters of CTs are mainly due to the effect of phase separation between LC-rich and polymer-rich area during exposure. The temperature effects on lasing properties of H-PDLC in CTs were also investigated. Our work verifies the possibility to achieve miniature laser devices in cylindrical confinement structures, such as CT, hollow-fiber or photonic crystal fiber, and extends the applicable scope of H-PDLC.

OCIS codes: (090.2890) Holographic optical elements; (140.2050) Dye lasers; (160.3710) Liquid crystals.

References and links

1. Y. J. Liu, Y. C. Su, Y. J. Hsu, and V. K. S. Hsiao, "Light-induced spectral shifting generated from azo-dye doped holographic 2D gratings," J. Mater. Chem. **22**(28), 14191–14195 (2012).
2. Y. J. Liu, X. W. Sun, H. I. Elim, and W. Ji, "Gain narrowing and random lasing from dye-doped polymer-dispersed liquid crystals with nanoscale liquid crystal droplets," Appl. Phys. Lett. **89**(1), 011111 (2006).
3. S. M. Xiao, Q. H. Song, F. Wang, L. Y. Liu, J. H. Liu, and L. Xu, "Switchable random laser from dye-doped polymer dispersed liquid crystal waveguides," IEEE J. Quantum Electron. **43**(5–6), 407–410 (2007).
4. Q. Song, L. Liu, L. Xu, Y. Wu, and Z. Wang, "Electrical tunable random laser emission from a liquid-crystal infiltrated disordered planar microcavity," Opt. Lett. **34**(3), 298–300 (2009).
5. F. F. Yao, H. T. Bian, Y. B. Pei, Ch. F. Hou, and X. D. Sun, "Behaviors of random laser in dye-doped nematic liquid crystals," Opt. Commun. **359**, 15–19 (2016).
6. W. B. Huang, Z. H. Diao, L. S. Yao, Z. L. Cao, Y. G. Liu, J. Ma, and L. Xuan, "Electrically Tunable Distributed Feedback Laser Emission from Scaffolding Morphologic Holographic Polymer Dispersed Liquid Crystal Grating," Appl. Phys. Express **6**(2), 022702 (2013).
7. Y. Nagai, R. Fujimura, and K. Kajikawa, "Core-resonance cylindrical whispering gallery mode laser of dye-doped nematic liquid crystal," J. Opt. Soc. Am. B **30**(8), 2233–2239 (2013).
8. Y. Matsuhisa, Y. Huang, Y. Zhou, S. T. Wu, R. Ozaki, Y. Takao, A. Fujii, and M. Ozaki, "Low-threshold and high efficiency lasing upon band-edge excitation in a cholesteric liquid crystal," Appl. Phys. Lett. **90**(9), 091114 (2007).

#260572 Received 7 Mar 2016; revised 23 Mar 2016; accepted 23 Mar 2016; published 28 Mar 2016

9. J. Etxebarria, J. Ortega, C. L. Folcia, G. Sanz-Enguita, and I. Aramburu, "Thermally induced light-scattering effects as responsible for the degradation of cholesteric liquid crystal lasers," Opt. Lett. **40**(7), 1262–1265 (2015).
10. A. Varanytsia, H. Nagai, K. Urayama, and P. Palffy-Muhoray, "Tunable lasing in cholesteric liquid crystal elastomers with accurate measurements of strain," Sci. Rep. **5**, 17739 (2015).
11. J. Kim, J. H. Suh, B. Y. Lee, S. U. Kim, and S. D. Lee, "Optically switchable grating based on dye-doped ferroelectric liquid crystal with high efficiency," Opt. Express **23**(10), 12619–12627 (2015).
12. S. M. Morris, A. D. Ford, M. N. Pivnenko, and H. J. Coles, "Electronic control of nonresonant random lasing from a dye-doped smectic A (*) liquid crystal scattering device," Appl. Phys. Lett. **86**(14), 141103 (2005).
13. W. Cao, A. Muñoz, P. Palffy-Muhoray, and B. Taheri, "Lasing in a three-dimensional photonic crystal of the liquid crystal blue phase II," Nat. Mater. **1**(2), 111–113 (2002).
14. S. T. Hur, B. R. Lee, M. J. Gim, K. W. Park, M. H. Song, and S. W. Choi, "Liquid-crystalline blue phase laser with widely tunable wavelength," Adv. Mater. **25**(21), 3002–3006 (2013).
15. J. H. Lin and Y. L. Hsiao, "Manipulation of the resonance characteristics of random lasers from dye-doped polymer-dispersed liquid crystals in capillary tubes," Opt. Mater. Express **4**(8), 1555–1563 (2014).
16. C. R. Lee, S. H. Lin, C. H. Guo, S. H. Chang, T. S. Mo, and S. C. Chu, "All-optically controllable random laser based on a dye-doped polymer-dispersed liquid crystal with nano-sized droplets," Opt. Express **18**(3), 2406–2412 (2010).
17. Y. J. Liu, X. W. Sun, P. Shum, H. P. Li, J. Mi, W. Ji, and X. H. Zhang, "Low-threshold and narrow-linewidth lasing from dye-doped holographic polymer-dispersed liquid crystal transmission gratings," Appl. Phys. Lett. **88**(6), 061107 (2006).
18. Z. H. Diao, W. B. Huang, Z. H. Peng, Q. Q. Mu, Y. G. Liu, J. Ma, and L. Xuan, "Anisotropic waveguide theory for electrically tunable distributed feedback laser from dye-doped holographic polymer dispersed liquid crystal," Liq. Cryst. **41**(2), 239–246 (2014).
19. W. K. Choi and Y. M. Li, "Vertically-Aligned Polymer Stabilized Liquid Crystals (VA-PSLC) with a Curing Voltage for Fast-Response Wavelength-Tuning Applications," Mol. Cryst. Liq. Cryst. **613**(1), 45–50 (2015).
20. L. K. Seah, V. M. Murukeshan, P. Wang, and Z. X. Chao, "Tunable external cavity laser based on liquid crystal fabry-perot interferometer and liquid crystal phase shifter," Int. J. Optomechatronics **1**(1), 63–72 (2007).
21. S. J. Woltman, G. D. Jay, and G. P. Crawford, "Liquid-crystal materials find a new order in biomedical applications," Nat. Mater. **6**(12), 929–938 (2007).
22. M. S. Li, A. Y. G. Fuh, J. H. Liu, and S. T. Wu, "Bichromatic optical switch of diffractive light from a BCT photonic crystal based on an azo component-doped HPDLC," Opt. Express **20**(23), 25545–25553 (2012).
23. Y. P. Huang, Y. M. Chang, T. Y. Tsai, and W. Lee, "H-PDLC/Clay Nanocomposites," Mol. Cryst. Liq. Cryst. (Phila. Pa.) **512**(1), 167–178 (2009).
24. D. Luo, X. W. Sun, H. T. Dai, H. V. Demir, H. Z. Yang, and W. Ji, "Temperature effect on the lasing from a dye-doped two-dimensional hexagonal photonic crystal made of holographic polymer-dispersed liquid crystals," J. Appl. Phys. **108**(1), 013106 (2010).
25. K.-Y. Yu, S.-H. Chang, C.-R. Lee, T.-Y. Hsu, and C.-T. Kuo, "Thermally tunable liquid crystal distributed feedback laser based on a polymer grating with nanogrooves fabricated by nanoimprint lithography," Opt. Mater. Express **4**(2), 234–240 (2014).
26. H. P. Tong, Y. R. Li, J. D. Lin, and C. R. Lee, "All-optically controllable distributed feedback laser in a dye-doped holographic polymer-dispersed liquid crystal grating with a photoisomerizable dye," Opt. Express **18**(3), 2613–2620 (2010).

1. Instruction

Lasing behaviors in dye-doped liquid crystals (LC) or LC-based materials have attracted much attention due to wide tunability high integration, low cost. Moreover, LC lasers have shown strong potential for various applications, such as spectroscopic light sources [1, 2], active displays [3], and optical communication [4], etc. Different types of LC materials, such as nematic [2, 3, 5–7], cholesteric [8–10], sematic [11, 12], blue phase LC [13, 14] and LC elastomer [10] have been exploited to generate tunable lasing actions. Other LC/polymer composites including polymer-dispersed LC [2, 3, 15, 16] (PDLC), holographic polymer-dispersed LC [1, 17, 18] (H-PDLC), and polymer-stabilized LC (PSLC) [19] have been also widely studied for tunable lasers. With the rapid development of micro-nano-science and technology, various types of microresonators have been developed, such as the Fabry-Perot cavity [20], distributed feedback (DFB) gratings [17, 18], photonic crystals [5], and random resonators [3–5]. As a result, the above mentioned LC and LC-based composite materials (nematic, cholesteric, blue phase, sematic, PDLC, H-PDLC, and PSLC etc.) can be filled into or self-form the resonators to improve or enhance the lasing properties.

#260572 Received 7 Mar 2016; revised 23 Mar 2016; accepted 23 Mar 2016; published 28 Mar 2016

Among the aforementioned material systems, H-PDLC has received particular interest due to its wide applications, such as bimolecular detectors [21], high-speed optical switch [11, 22], and organic lasers [6, 17]. The performance of H-PDLC can also been enhanced with nanoparticles doping [23]. With holographic technology, the organic grating structures can be photo-solidified in the LC/polymer composite, which are immovable, but with flexibility. Therefore, H-PDLC devices can provide not only highly integratable capability with variety of geometric configurations, but also excellent stability compared to the completely fluidic LC based devices. Until now, tunable lasing properties from H-PDLC gratings in planar cells have been investigated extensively, such as electrical [6], thermal [24, 25], and optical [26] tunable methods. As aforementioned the flexibility of H-PDLC, of interest is what's the lasing properties when the H-PDLC grating structures are prepared in a cylindrical geometry, such as photonic crystal fiber, micro capillary etc.. Furthermore, the 2-D cylindrical devices can be easily integrated as array architecture for various applications. Additionally, H-PDLC structures with various grating pitches in cylindrical geometry can be integrated as an array to form a laser array with multicolor emission under the same pumping source.

In this paper, we assembled H-PDLC in 2-D confinement single core capillaries, and then studied the lasing properties from H-PDLC in CTs with various core diameters (75 μm, 100 μm, and 300 μm). Experimental results show the lasing emission peak is mainly determined by the grating period of H-PDLC regardless the core diameters, whereas the lasing thresholds decrease with large core diameters. Furthermore, we also discuss the Q-factor of the lasing cavity of H-PDLC in CTs. At last, effects of temperature on the lasing properties of H-PDLC in CTs were investigated as well.

2. The preparation of dye-doped H-PDLC in capillary

As reported in other literatures, pre-polymer syrup was prepared first, which consists of penta-functional dipentaerythritol hydroxyl pentaacrylate (DPHPA, 29%), chain extender N-vinyl pyrrolidinone (NVP, 10 wt%), coinitiator N-phenylglycine (NPG, 0.8 wt%), photoinitiator Rose Bengal (RB, 0.1 wt%) and laser dye 4-(dicyanomethylene)-2-methyl-6-(p-dimethylaminostyryl)-4Hpyran (DCM, 0.1 wt%) all from Sigma-Aldrich, nematic LC E7 (n_o = 1.521, n_e = 1.746, 31%) from Merck, monomer phthalic diglycol diacrylate (PDDA, 29 wt%) from Xiya Reagent. The syrup was mixed about 6 hours at 40°C in the dark to form a homogeneous mixture. The syrup was then filled into quartz capillaries (TSP010150, Polymicro Technologies Inc.), which were processed in concentrated sulfuric acid in ultrasonic cleaner to get rid of the polyimide coating and carved up as 5 cm by the fiber laser. In our experiments, capillaries with three different core diameters (75 μm, 100 μm, and 300 μm) were adopted, which were marked as CT I, CT II and CT III respectively. The wall thicknesses of our capillaries are all 300 μm.

Figure 1 shows the experimental configuration to record the hologram pattern in the capillary tube. A collimated laser beam (532 nm) is split into two beams with beam splitter and recombined at the tube with a mirror. To enhance the light coupling efficiency and minimize the error, the CTs were sandwiched between two glass plate filled with index matching liquid. After exposure, LC-rich and polymer-rich alternating regimes formed due to photo-polymerization induced phase separation, as shown in the magnified inset in Fig. 1. As a result, the alternating refractive index modulation also formed inside the structure. In our experiment, the exposure intensity of each beam for all the samples was about 8mW/cm^2 and the exposure time was 3 min, which had been optimized to achieve high diffraction efficiency H-PDLC structures.

Furthermore, the sample was post cured for 10 min by UV exposure machine (HT-3000) to stabilize the polymerization. For CTs I-III, the intersect angles between two beams are all 53.7°.

#260572 Received 7 Mar 2016; revised 23 Mar 2016; accepted 23 Mar 2016; published 28 Mar 2016

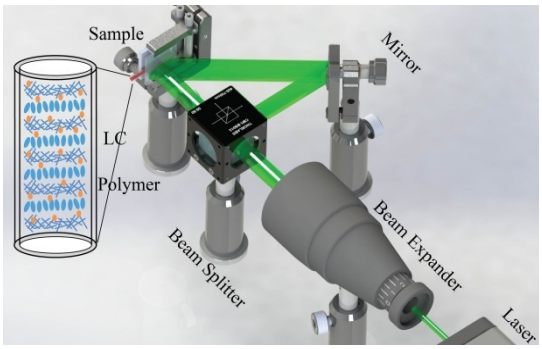

Fig. 1. Schematic to fabricate the grating structures in capillary tubes.

Theoretically, grating pitch (Λ) is determined by the angle (θ) between the recording beams according to the following formula:

$$\Lambda = \frac{\lambda_r}{2\sin\frac{\theta}{2}} \tag{1}$$

where λ_r is the recording wavelength at 532 nm, θ is the angle between the two beams. Therefore, the calculated grating pitch for all CTs I-III is about 589 nm.

To verify the grating formation in CTs, a large pitch grating was prepared first by tuning the intersecting angle between two beams (about 15.3°). Figure 2(a) shows the grating image in the capillary tube under the polarization optical microscope (POM). As labeled in Fig. 2(a), the period of grating is about 2 μm. It verified that the grating structures could be generated effectively in CTs by means of holographic method.

Furthermore, an H-PDLC cell in planar glass cell was prepared to check the formation of grating with small pitch. After exposure, the H-PDLC cell was split in liquid nitride. After washing out LC contents by soaked the H-PDLC film in isopropanol for 12 h, a pure polymer film was pasted on one substrate for further SEM measurement. Figure 2(b) shows morphology of the dye-doped H-PDLC grating with the scanning electron microscope (SEM), which clearly reveals a uniform grating structure with the grating period is about 550nm, the small difference between the measurement and calculated value is ascribed to the shrinkage of the prepolymer during polymerization procedure.

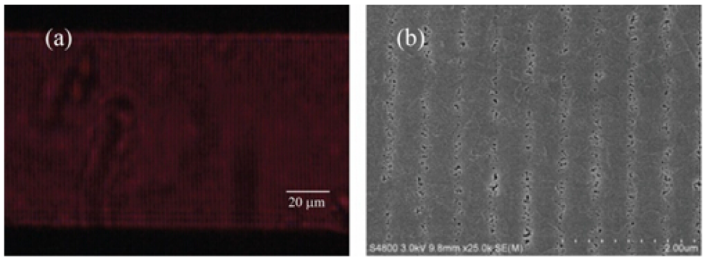

Fig. 2. (a) Grating image in the capillary tube under the polarization optical microscope (POM) (b) SEM image showing the surface morphology of the dye-doped H-PDLC grating.

3. The lasing properties of dye-doped H-PDLC in capillary

First, the absorption and photoluminescence spectra of the DCM-doped films are measured to ensure the effect light absorption and emission. As shown in Fig. 3, the absorption range (by a UV-Vis UV3600) of the film is from 400 nm to 800 nm with absorption peak at 480 nm. The emission range (USB4000, Ocean Optics Inc., USA) of the film is from 550 nm to 750 nm

#260572 Received 7 Mar 2016; revised 23 Mar 2016; accepted 23 Mar 2016; published 28 Mar 2016

and the emission peak is at 615 nm, which overlaps the absorption band in the spectral range of 550–700 nm.

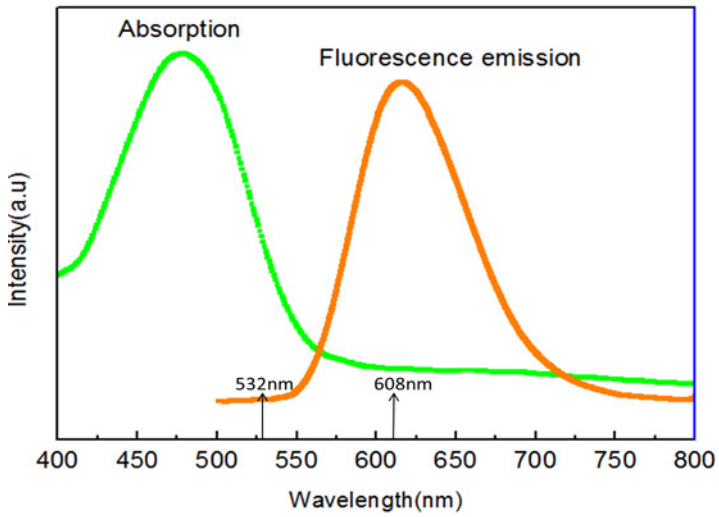

Fig. 3. The absorption and fluorescence emission spectra of DCM doped HPDLC films.

Figure 4 shows the experimental setup to explore the lasing performance of H-PDLC in capillary. The dye-doped HPDLC were pumped by Q-switched frequency doubled Nd:YAG laser with a repetition rate of 10 Hz and a pulse width of 10 ns. The laser beam was focused on capillary surface by a cylindrical lens to ensure sufficient distributed feedback gain.

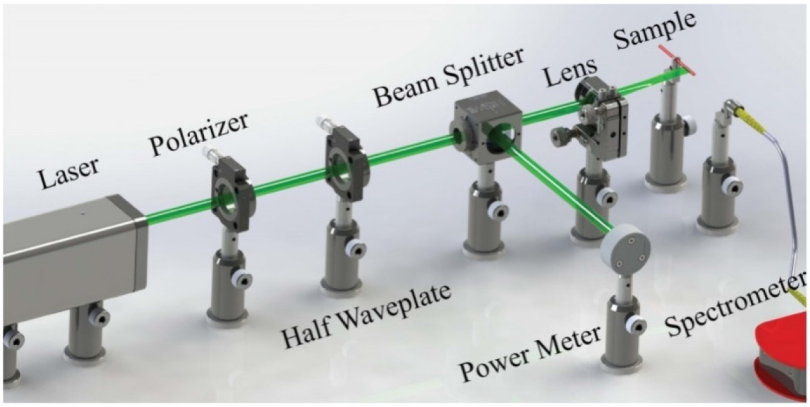

Fig. 4. Schematic diagram of the experimental setup for emission laser in dye doped HPDLC, which provides the feedback for laser oscillations.

The axial emission spectrum from the capillary tube was collected by the fiber tip and measured by the optical spectrometer (AvaSpe-ULS3648TEC-USB2 resolution about 0.3 nm, Avantes Inc.). Figure 5 shows the emission properties of the dye-doped H-PDLC in capillaries with different core diameters. Under low pump energy, broad spontaneous spectra were observed from all the samples, which resembled the spontaneous emission of DCM molecules. When the pulse energy was larger than certain value, much narrower spikes appeared on the top of the spontaneous emission spectrum, i.e. the lasing emission from the H-PDLC filled in CTs.

The output lasing wavelength is decided by Bragg equation:

#260572 Received 7 Mar 2016; revised 23 Mar 2016; accepted 23 Mar 2016; published 28 Mar 2016

$$\lambda_{las} = 2n_{eff}\Lambda / m \tag{2}$$

where m is the Bragg order and n_{eff} is the effective refractive index of the materials. In our experiment, the grating pitch is 589 nm, the effective refractive indices n_{eff} was about 1.55, which was calculated as [6]:

$$n_{eff} = \left[n_p{}^2 \times \varphi_p + n_{eff\_LC}^2 \times \varphi_{LC} + \left(2n_o^2/3 + n_e^2/3\right) \times \left(1 - \varphi_p - \varphi_{LC}\right) \right]^{1/2} \tag{3}$$

where, n_p = 1.541is refractive index of the pure polymer, φ_p = 0.69 is volume proportion of the pure polymer, φ_{LC} = 0.12 is volume proportion of the phase-separated LCs, and $1\text{-}\varphi_p\text{-}\varphi_{LC}$ are the volume proportions of the LCs dissolved in the polymer.

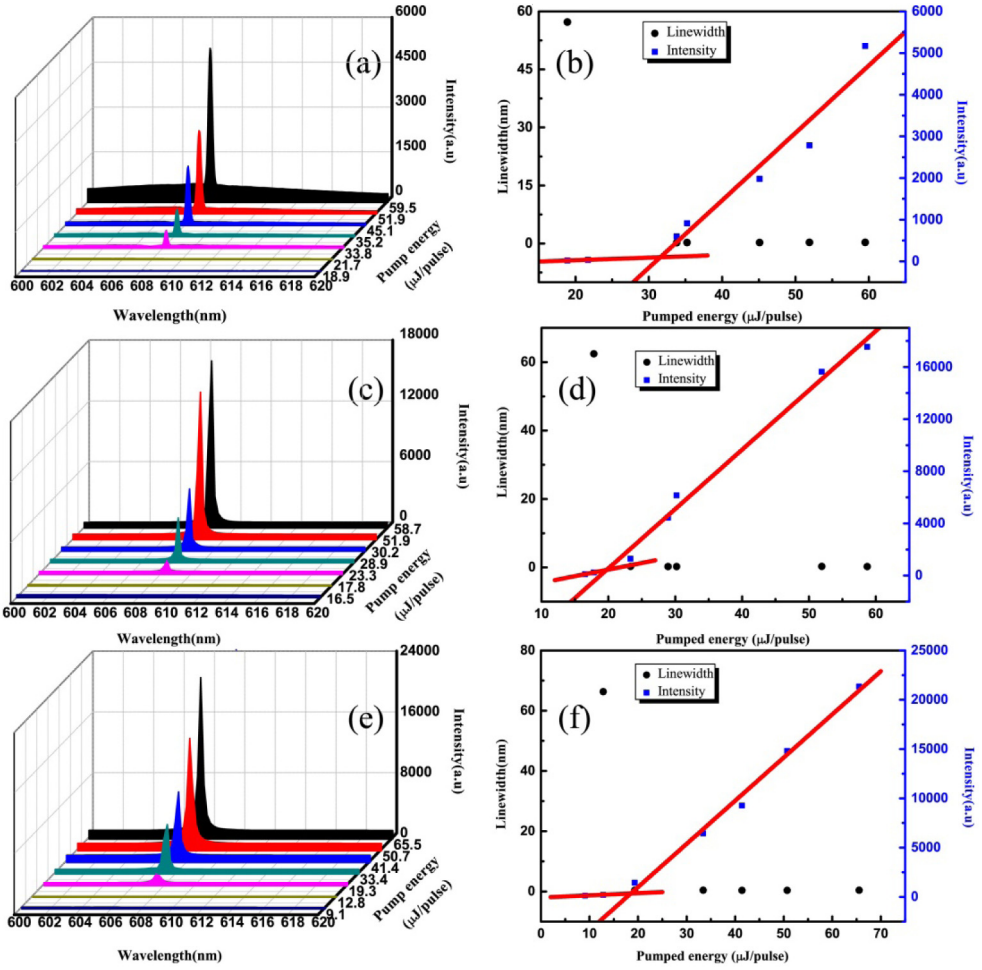

Fig. 5. Evolution of the emission spectra with various pump energy from H-PDLCs inside the single core capillary with core diameter of (a) 75 μm (CT I), (c) 100 μm (CT II), and (e) 300 μm (CT III); relative peak intensities and FWHMs of emission spikes with various pump energy from (b) CT I, (d) CT II, and (f) CT III.

To investigate the emission properties of H-PDLCs in capillaries, the evolution of emission spectra, relative intensities and FWHMs of lasing peaks are collected in Fig. 5. Figures 5(a), 5(c) and 5(e) show the evolution of emission spectra with the pump energies, by which the locations of emission peaks can be calculated. It is obvious the lasing behavior

#260572 Received 7 Mar 2016; revised 23 Mar 2016; accepted 23 Mar 2016; published 28 Mar 2016

occurs when the pump energy larger than a certain value, i.e. lasing threshold. For the three capillaries in our experiment, the thresholds are different as well. The emission peaks are located at 608.2 nm, 608.4 nm and 607.4 nm, which correspond to CT I, II and III respectively. The slight discrepancy of the lasing peaks can be mainly attributed to the difference of grating pitch and the effective index modulation. As the grating structures in CTs are formed by means of phase separation, the exposure conditions affect the phase separation results and thus lead to various lasing performance. In our experiment, similar exposure conditions are adopted (exposure time, incident light intensity and intersect angle) for all the samples. Meanwhile, the different core diameters intrinsically lead to different prepolymer thickness, which presents varied exposure dose in H-PDLC. Consequently, the grating pitch or effective index shows slight difference with varied core diameters and results in peak shift. Especially for CT III, the diameter is too large (300 μm) to keep uniform exposure intensity along the cross section of the tube, and the large shrinkage after post curing leads to a large peak shift (~1 nm).

Furthermore, as shown in Figs. 5(b), 5(d) and 5(f), after curve fitting the spectra data, the corresponding FWHMs of CT I-III are 0.29, 0.32, and 0.42 nm respectively. It is clear that the FWHMs of emission peaks increase with increasing the core diameters. This effect can be ascribed to the phase separation level as mentioned before. In CT I, the small diameter means the thinner thickness of prepolymer, therefore, the uniform intensity distribution in CT I can be achieved and results in relative complete phase separation. At last, the high quality H-PDLC grating due to complete phase separation enables the narrow FWHM of emission peak.

Subsequently, according to Figs. 5(b), 5(d) and 5(f), the thresholds of the H-PDLC in CTs are 31.5, 23.1 and 19.4 μJ/pulse for CT I, CT II and CT III, respectively. The thresholds decrease with the increasing core diameters. The lower laser threshold is due to the high pump energy in CTs with large core diameters. As shown in Figs. 6(a)-6(c), the small core diameter (smaller than the FWHM of focal line of pump laser) can't absorb all the incident light energy, therefore, more energy required to keep sustained lasing output. Therefore, the pump energy can be utilized effectively to convert to lasing energy in CTII and III. From the experimental images for CTs I-III as shown in bottom row in Figs. 6(a)-6(c), the intensities of emission light from CT II and III are significantly brighter than that of CT I. In our experiment, the FWHM of focal line of pump laser is about 80 μm. The diameter of CT I is smaller than the FWHM of focal line. For CT II and III, FWHMs of focal line are smaller than inner diameters of CTs. At the same time, we have measured the fluorescence emission spectra of different diameter capillaries with same energy as shown in Fig. 6(d), it is clear that highest fluorescent intensity emitting from CT III. Finally, we have to emphasize that the outer shell of CT may disturb or enlarge the focal line. The real threshold of CT II, therefore, is larger than CT III. For CT III, the inner diameter is thicker and all the pumped energy can be absorbed to support the lasing output. Consequently, the threshold of CT III is lowest.

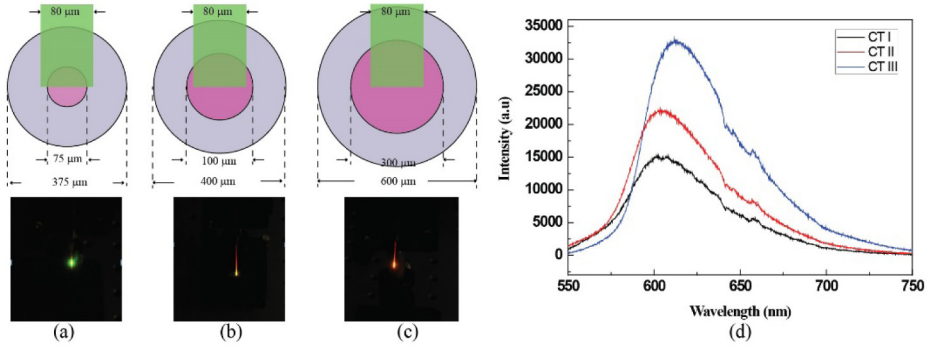

Fig. 6. Schematic of geometric relation between pumped light and capillary for (a) CT I, (b) CT II and (c) CT III and the recorded experimental images (bottom row).

#260572 Received 7 Mar 2016; revised 23 Mar 2016; accepted 23 Mar 2016; published 28 Mar 2016

We also calculated the quality factor Q of H-PDLC in CT cavity, which is determined by expression as below:

$$Q = \frac{\lambda_{las}}{\Delta\lambda} \tag{4}$$

where λ_{las} is the central laser wavelength emitted from the grating, and $\Delta\lambda$ is the spectrum FWHM of the output lasing.

Table 1 lists the lasing emission wavelength λ_{las}, FWHM ($\Delta\lambda$) and the estimated Q-factor for different CTs cavities with different core diameters. The Q-factor of the CT I is highest (about 2027), which means the relative complete phase separation and the formation of high quality grating in CT I. As core diameter increases to 300 μm, the measured FWHM increases to about 0.42 nm and the Q-factor declines to about 1446, which indicates the large prepolymer thickness has side effect on the phase separation.

Table 1. the peak wavelength, FWHM,and the estimated *Q*-factor from capillary tubes

	CT I	CT II	CT III
λ_{las}	608.2	608.4	607.4
$\Delta\lambda$	0.29	0.32	0.42
Q	2097	1901	1446

As we know, the temperature can affect the order parameter of LC director, therefore influence the effective index of LC. Initially, the thermal effect of pumped laser (nanosecond pulsed laser) was considered. A H-PDLC CT III had been pumped with fixed energy (60 μJ/pulse) for 40 min. Experimental results (not shown here) showed that the wavelength of lasing emission didn't change with prolonged pumping time. But the emission intensity decreased with lasting pump, which was due to the bleach of laser dye (DCM) after a long time excitation. It is concluded that the thermal effect of pumped laser (low energy but larger than lasing threshold) on lasing performance can be omitted.

Finally, the effects of temperature on the lasing properties from H-PDLC in CTs were explored by heating sample directly. H-PDLC in CT III was adopted and pumping energy was kept as 60 μJ/pulse. When increasing the temperature from T = 21 °C to T = 56 °C, the lasing peaks had blue-shift from λ = 607.4 nm to λ = 595.6 nm, while the emitting intensity decreased. Meantime, the FWHMs of lasing peaks increased with higher temperature. The results were shown in Fig. 7. The blue-shift of emission wavelength is attributed to the decease of effective index of LC-rich layer in H-PDLCs induced by the response of LC director alignment for temperature. This blue-shift effect is coincident with the reported results in Ref [25].

#260572 Received 7 Mar 2016; revised 23 Mar 2016; accepted 23 Mar 2016; published 28 Mar 2016

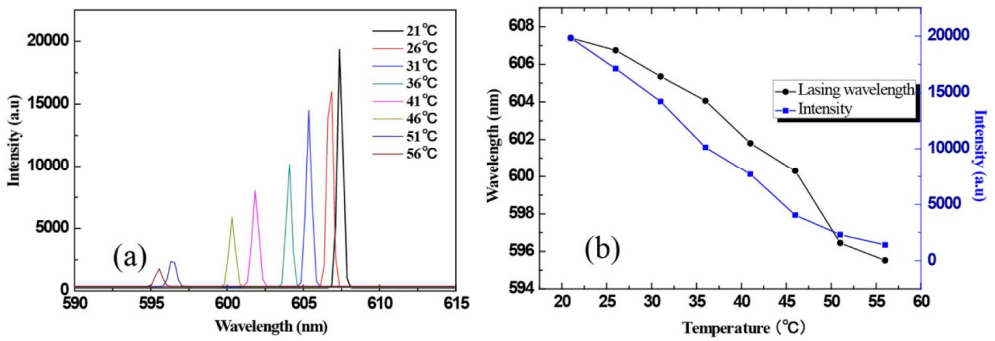

Fig. 7. The temperature effects on the lasing performance of H-PDLC in CTs. (a) denotes the lasing peaks with varied temperatures and (b) shows the wavelengths and intensities of emission lasers.

3. Conclusion

In this work, H-PDLCs have been successfully prepared in CTs by means of double-beam interference. Moreover, lasing behaviors from dye-doped H-PDLC in CTs, such as lasing emission peaks, lasing thresholds, and FWHMs of emission peaks, have been also explored experimentally. With the same experimental configurations (exposure time, intensity and intersection angle between two beams), lasing thresholds increased with decreasing core diameters of CTs. While the FWHMs of lasing peaks increased with large core diameters. These effects were mainly attributed to the degree of the phase separation between LC and polymer influenced by the core diameters of CTs. Experimental results also showed the blue-shift of lasing peaks with increased temperature, which could be attributed to the decreased effective index of LC-rich layer in H-PDLC. The method to prepare H-PDLC in capillary tubes can be extended to other 2-D cylindrical geometry, such as hollow optical fiber or photonic crystal fiber, and enable miniaturized tunable laser sources for different geometric configurations.

Acknowledgments

This work was supported in part by the National Natural Science Foundation (Grant No.11535008, 61405088, 61177061); Key project of Nature Science Foundation of Tianjin No.14JCZDJC31400.

#260572 Received 7 Mar 2016; revised 23 Mar 2016; accepted 23 Mar 2016; published 28 Mar 2016